Practical Implementation and Adaptation of Rainforest-Based Inter-calibration for ESCAT-ASCAT Scatterometer Data Records

Clay Harrison[1], Sebastian Hahn[1], Roland Lindorfer[1], Thomas Melzer[1], Raffaele Crapolicchio[2], Wolfgang Wagner[1]

[1] TU Wien, Department of Geodesy and Geoinformation, Vienna, Austria
(clay.harrison, sebastian.hahn, roland.lindorfer, thomas.melzer, wolfgang.wagner)@geo.tuwien.ac.at
[2] Serco Italia SpA - for European Space Agency, Rome, Italy

Keywords: scatterometer; calibration; ERS; ASCAT; backscatter; rainforest;

Abstract

C-band scatterometers have been collecting radar backscatter data since 1991, providing valuable long-term records for environmental monitoring applications such as soil moisture and vegetation dynamics. However, differences in sensor calibration between missions introduce biases that compromise the continuity of these data records. This paper presents the practical implementation and adaptation of Reimer’s (2014) rainforest-based inter-calibration approach for ESA’s ERS satellites (ESCAT) and Metop/ASCAT instruments. We implement the method as a modern, open-source Python framework and apply it to the newly complete ERS data record (including ERS-1 data not available in the original study). The resulting calibrated backscatter data record will enable improved long-term monitoring of land surface dynamics with reduced mission-to-mission variability in bias and slope response over incidence angle.

1. Introduction

Long-term satellite observations are essential for understanding environmental change and supporting climate monitoring applications. C-band fan-beam scatterometer missions, spanning from the 1991 launch of ERS-1 through the continuing Metop series, provide one of the longest continuous records of surface backscatter observations available for environmental monitoring. These observations form the foundation for numerous applications including soil moisture retrieval (Scipal et al., 2002; Bartalis et al., 2007), vegetation dynamics assessment (Wagner et al., 1999), and climate trend analysis (Wagner et al., 2013).

However, creating a truly continuous data record across multiple satellite missions presents significant technical challenges due to differences in calibration procedures and operational characteristics. Significant prior work has been done to develop robust calibration methods for the C-band scatterometers onboard ERS and Metop.

In particular, Reimer (2014) established a methodological foundation for rainforest-based intra- and inter-calibration of data from multiple scatterometer missions, but that work was limited to Metop-A and ERS-2 data available at the time, and did not analyze the complete ERS record now available. Furthermore, the original implementation was not publicly available or maintained for operational use, limiting its practical applicability.

So, when European Space Agency recently completed the reprocessing of the entire ERS mission data using the ASPS system, including the previously unavailable ERS-1 record and significant new additions to the ERS-2 record, this necessitated a practical implementation of Reimer’s method to create a continuous, inter-calibrated climate data record.

This study addresses these gaps by (i) implementing Reimer’s (2014) methodological framework in a modern, open-source Python environment optimized for large-scale data processing, (ii) expanding the analysis to include the complete ERS dataset, including ERS-1 and late-period ERS-2 data, and (iii) evaluating which components of the original methodology provide value for this expanded dataset. Our experience reveals that certain methodological components (specifically the intra-calibration step) can potentially add complexity without commensurate improvement when working with the reprocessed ASPS data.

The resulting calibrated backscatter data record enables improved long-term monitoring of land surface dynamics with reduced mission-to-mission variability in bias and slope response over incidence angle. This is particularly valuable for applications requiring consistent backscatter time series, such as soil moisture retrieval and vegetation dynamics assessment. For soil moisture monitoring specifically, consistent C-band backscatter observations are fundamental for reliable trend analysis across the full 1991-present period.

2. Background and Related Work

The calibration of satellite scatterometer observations has been extensively studied since the early operational missions. Long and Skouson (1996) established the theoretical foundation for using tropical rainforests as natural calibration targets by demonstrating that these regions exhibit azimuthal isotropy and temporal stability when seasonal variations are accounted for. This approach exploits the unique characteristics of dense rainforest canopies, which provide relatively constant backscatter responses under varying viewing geometries.

Reimer (2014) extended the rainforest calibration approach to address multi-mission scatterometer data harmonization. The proposed framework consists of two primary stages: (1) intra-calibration to ensure temporal consistency within each individual mission, and (2) inter-calibration to harmonize measurements between missions using natural reference targets. The method employs polynomial corrections to account for systematic differences in both absolute backscatter levels and incidence angle response characteristics.

This contribution has been peer-reviewed. The double-blind peer-review was conducted on the basis of the full paper.
https://doi.org/10.5194/isprs-annals-XI-3-2026-411-2026

Several factors motivated the need to re-implement and adapt this methodology:

- **Expanded Data Availability:** The complete ERS record (including ERS-1 and late-period ERS-2 data) was not available in the original study
- **Processing Environment:** Modern Python-based processing provides advantages in scalability, reproducibility, and community accessibility
- **Computational Efficiency:** Processing multiple decades of global data requires optimized approaches

3. Implementation Approach

We implemented the calibration framework in Python, leveraging xarray and dask for efficient parallel processing. The implementation is structured as an open-source toolkit designed for reproducibility, replacing the original IDL-based approach which was no longer maintained for operational use. The framework emphasizes scalability for processing large multi-decadal, multi-mission scatterometer data records.

The calibration workflow is organized into discrete stages to ensure systematic processing and facilitate debugging. The pipeline begins with raw ASPS/Metop data ingestion, proceeds through quality filtering and target selection, computes calibration parameters, and finally applies corrections to the full data record. Each stage maintains logging and intermediate checkpoints to enable reproducibility and diagnostic assessment.

4. Data and Quality Control

4.1 Dataset Overview

This study utilizes C-band backscatter data from ESA’s *European Remote Sensing* (ERS-1 and ERS-2) satellites and the Metop-A *Advanced Scatterometer* (ASCAT). The ERS and Metop missions provide complementary long-term scatterometer observations spanning 1991 to present, enabling the construction of multi-decadal backscatter time series for environmental monitoring applications such as soil moisture retrieval and vegetation dynamics assessment.

Both ESCAT and ASCAT employ fan-beam antenna configurations. ESCAT instruments onboard ERS-1 and ERS-2 acquire backscatter triplets at incidence angles ranging from 25 to 55°, while ASCAT covers 35 to 65°. All data were obtained from an institutional scatterometer archive and resampled from the native swath geometry onto a 12.5 km global Fibonacci grid to ensure spatial consistency between sensors (Hahn and Harrison, 2025).

4.2 Data Quality

To ensure that the calibration process accurately characterizes each backscatter time-series and the differences between them, we take several quality-control steps which address instrument-specific characteristics, data completeness, and geometric consistency concerns.

All available instrument-specific quality flags were applied to the ERS scatterometer data, restricting analyses to observations meeting mission-defined data quality standards.

Only complete backscatter triplets—where all three measurement beams (fore, mid, aft) provided valid observations simultaneously—were retained from both ERS and Metop instruments. Additionally, backscatter measurements based on fewer than fifty echoes were discarded.

To facilitate direct comparison between the different sensor geometries, observations were constrained to the overlapping incidence angle ranges common to both instrument systems: 35–55° for the fore and aft beams and 25–45° for the mid beam. Furthermore, only observations from right-side swath of Metop-A ASCAT were used during inter-calibration, in order to maintain consistency with the single-swath configuration of the ERS instruments.

Based on documented mission anomalies and previous calibration assessments, we excluded ERS-2 data collected after 2001 when computing ERS-2/Metop-A inter-calibration parameters to avoid contamination by known instrument issues. These problems began with the gyroscope failure in January 2001, which altered the satellite’s attitude control system and led to increased orbital variability and irregular viewing geometries. Subsequently, the onboard tape recorder failed in June 2003, with the result that after this time, data could only be collected when the satellite was in range of a ground station. These technical issues significantly affected the measured backscatter values and necessitated the exclusion of these periods from calibration parameter estimation.

4.3 Natural Target Selection Criteria

Following the established methodology, we selected natural targets in ESCAT data based on three criteria: azimuthal isotropy, temporal stability, and spatial homogeneity of backscatter measurements. We analyzed data from the Amazon, Congo, Upper Guinea, and three Southeast-Asian (Borneo, Sumatra, Malaysia) rainforests over each satellite’s complete operational period to find Fibonacci grid points for which observed backscatter measurements fulfill all three criteria. The specific criteria thresholds applied for each satellite are summarized in Table 2, while the reference periods used for backscatter calibration are listed in Table 3. The selected natural calibration targets are illustrated in Figure 2, and the number of grid points selected by region and satellite is provided in Table 1.

The Amazon and Congo rainforests were designated as calibration regions due to their large spatial extent and the abundance of stable grid points available for robust parameter estimation. The Upper Guinea and SE Asian rainforests serve as independent validation regions to assess the generalizability of the derived calibration parameters. This spatial separation between calibration and validation regions ensures that validation results are not simply reflecting the same data used to estimate the calibration coefficients.

Azimuthal Anisotropy Assessment: Calculation of azimuthal anisotropy $\delta(L)$ at each grid point L follows Reimer (2014):

$$\delta_{O,S}(L,t_i) = \sigma^0_{F,O,S}(L,t_i) - \sigma^0_{A,O,S}(L,t_i) \tag{1}$$

$$\delta_{O,S}(L) = \left| \frac{1}{n} \sum_{i=1}^{n} \delta_{O,S}(L,t_i) \right| \tag{2}$$

$$\delta(L) = max(\delta_{O,S}(L)) \quad (3)$$

Where O is orbit direction (ascending/descending), S is swath (left/right, only applicable to ASCAT), L is the location (Fibonacci grid point), t_i is the time of observation i, and n is the total number of observations at location L.

Temporal and Spatial Variability Assessment: An estimate of long-term mean backscatter was calculated by first normalizing the observations to a reference incidence angle of 40°. For each location (grid point) L and azimuth configuration ϕ_j, we modeled the incidence angle dependence as follows:

$$\sigma^0(L, \theta, \phi_j) = B_0(L, 40^\circ, \phi_j) + B_1(L, 40^\circ, \phi_j) \cdot (\theta - 40^\circ) \quad (4)$$

where θ is the incidence angle, B_0 represents the backscatter at the reference angle, and B_1 is the slope parameter. Individual observations were normalized to 40° using:

$$\sigma^0(L, t_i, 40^\circ, \phi_j) = \sigma^0(L, t_i, \theta, \phi_j) - B_1(L, 40^\circ, \phi_j) \cdot (\theta - 40^\circ) \quad (5)$$

The long-term mean backscatter estimate for each grid point was then computed as the average of B_0 across all azimuth configurations:

$$\overline{\sigma^0}(L, 40^\circ) = \frac{1}{n_{\text{azimuth}}} \sum_{j=1}^{n_{\text{azimuth}}} B_0(L, 40^\circ, \phi_j) \quad (6)$$

To assess temporal stability, we calculated the variance of normalized backscatter for each azimuth configuration.

$$\nu^2(L, 40^\circ, \phi_j) = \frac{1}{n} \sum_{i=1}^{n} (\sigma_i^0(L, t_i, 40^\circ, \phi_j) - B_0(L, 40^\circ, \phi_j))^2 \quad (7)$$

The overall temporal variability parameter ν was then determined as the pooled standard deviation across all azimuth configurations:

$$\nu(L, 40^\circ) = \sqrt{\frac{\sum_{j=1}^{n_{\text{azimuth}}} n_j \cdot \nu^2(L, 40^\circ, \phi_j)}{\sum_{j=1}^{n_{\text{azimuth}}} n_j}} \quad (8)$$

where n_j is the number of observations used from azimuth configuration ϕ_j.

Observations for grid points fulfilling the azimuthal anisotropy and temporal variability criteria were kept, and the rest were discarded.

Using the remaining data, spatial variability of grid points within natural targets was evaluated using mean-shift clustering. In brief, the most probable mean backscatter coefficient $\overline{\sigma^0}(L, 40^\circ)$ within each target region is estimated from a probability density function, then grid points L with $\overline{\sigma^0}(L, 40^\circ)$ deviating from that mode value by less than the backscatter homogeneity threshold are selected for use in calibration.

Table 1. Number of grid points selected by region and satellite

Region	Satellite	Grid Spacing	# Grid Points
Amazon	ERS-1	12.5,km	14986
Amazon	ERS-2	12.5,km	14660
Amazon	Metop-A	12.5,km	13031
Congo	ERS-1	12.5,km	6174
Congo	ERS-2	12.5,km	6115
Congo	Metop-A	12.5,km	6281
SE Asia	ERS-1	12.5,km	2383
SE Asia	ERS-2	12.5,km	1990
SE Asia	Metop-A	12.5,km	2063
Upper Guinea	ERS-1	12.5,km	604
Upper Guinea	ERS-2	12.5,km	582
Upper Guinea	Metop-A	12.5,km	748

Table 2. Criteria for selection of natural targets.

Criterion	**ERS limit**	**Metop limit**
Azimuthal anisotropy	0.3,dB	0.2,dB
Temporal variability	0.4,dB	0.4,dB
Spatial backscatter variability	0.15,dB	0.15,dB

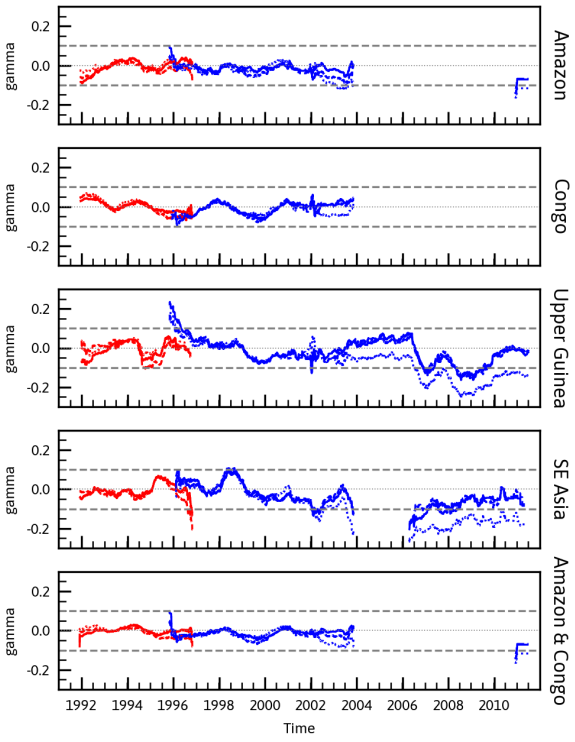

Figure 1. Deviation of gamma-nought backscatter daily means from seasonal means over time over different natural target regions (ERS-1 in red, -2 in blue; fore-beam: solid, mid-beam: dashed, aft-beam: dotted).

5. Calibration Method and Adaptations

We implemented the established rainforest-based intercalibration approach (Reimer, 2014), which uses stable natural targets as calibration references for harmonizing multi-mission scatterometer observations. The method assumes temporal stability of rainforest backscatter after removing seasonal cycles,

This contribution has been peer-reviewed. The double-blind peer-review was conducted on the basis of the full paper.
https://doi.org/10.5194/isprs-annals-XI-3-2026-411-2026 | © Author(s) 2026. CC BY 4.0 License.

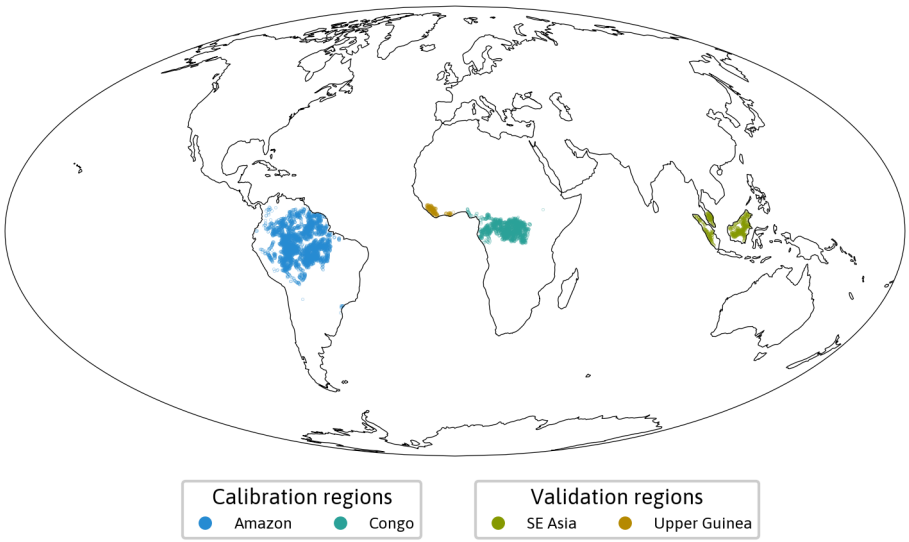

Figure 2. Selected natural calibration targets

enabling derivation of correction parameters to align sensor measurements.

5.1 Reference Backscatter Modeling

We characterize the expected backscatter response over each calibration target using polynomial modeling of data from a year-long reference period that has been determined to be relatively radiometrically stable (Table 3 lists the reference periods used for each satellite).

Prior to polynomial fitting, standard climatological normalization procedures are applied to remove predictable seasonal vegetation dynamics while preserving long-term backscatter characteristics.

After seasonal correction, reference backscatter characteristics are modeled as second-degree polynomials with respect to incidence angle:

$$\begin{aligned} \overline{\sigma^0}(L_T, \theta) = \\ B_0(L_T, 40^\circ) \\ +B_1(L_T, 40^\circ) \cdot (\theta - 40^\circ) \\ +B_2(L_T, 40^\circ) \cdot (\theta - 40^\circ)^2 \end{aligned} \tag{9}$$

where L_T is the target location, θ is the incidence angle, and B_0, B_1, B_2 are polynomial coefficients representing expected backscatter response over the target.

Table 3. Reference periods for backscatter calibration of ERS-1 and ERS-2 to Metop-A.

Satellite	Reference period
ERS-1	1992-05-01 - 1993-04-30
ERS-2	1998-01-01 - 1998-12-31
Metop-A	2007-01-01 - 2007-12-31

5.2 Intra-calibration of ERS-1 and 2

The intra-calibration procedure involves modeling temporal variations within each satellite’s record to ensure internal consistency. Following the original methodology, this would require: (1) dividing each satellite’s time series into regular periods (e.g. monthly), (2) computing differences between observed backscatter and the reference polynomial model for each calibration region and azimuth configuration, (3) fitting first-degree polynomials to these differences to derive time-varying bias and slope parameters, and (4) applying weighted averaging across calibration regions to minimize geophysical influences. This process generates a time series of correction parameters for each beam and orbit direction designed to correct temporal anomalies and improve beam-to-beam alignment (Reimer, 2014).

Omission of Intra-calibration: During testing of the intra-calibration step, we found that the ASPS reprocessed ERS data already exhibited good temporal stability over rainforest targets (instability not exceeding 0.033dB) outside of periods already known to be unstable (e.g. from the failure of ERS-2’s gyroscopes and onward) (Figures 1, 3). We were unable to verify that the computed intra-calibration parameters for this period represented actual changes in satellite calibration rather than subtle geophysical effects.

Furthermore, due to tape recorder failure in 2004, most of the ERS-2 data record does not have sufficient coverage over the Amazon and the Congo rainforests to generate stable intra-calibration coefficients using the existing methodology (Figure 3).

Therefore, to avoid the risk of overcorrection during periods which already have quite good temporal intra-calibration, and because calibration of ERS-2 data post-tape-recorder failure will require significant adjustment to the existing calibration strategy, we have decided to skip the intra-calibration step for the first version of the ASCAT-calibrated ESCAT backscatter data record.

5.3 Inter-calibration between ERS-1/2 and Metop-A

For each filtered observation from the ERS datasets, we compute the difference between observed backscatter and the corresponding Metop-A ASCAT reference (based on incidence angle, orbit direction, and region). These differences are charac-

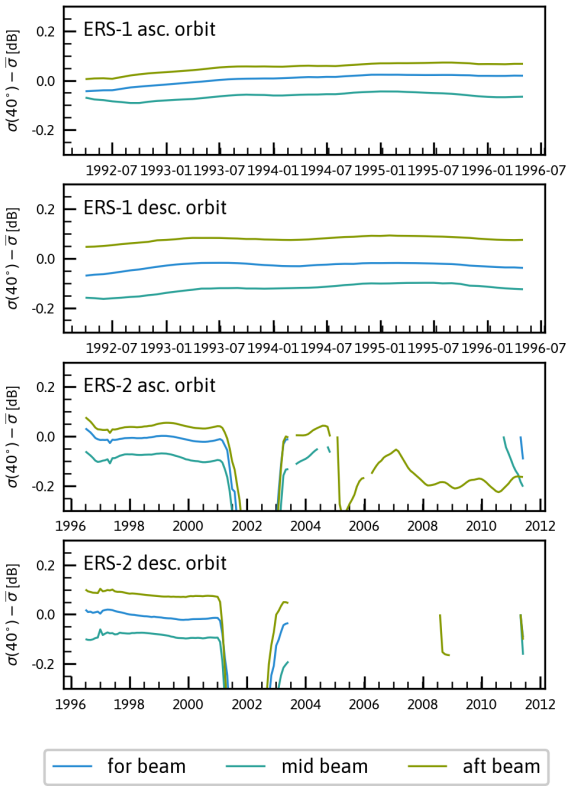

Figure 3. Computed intra-calibration value at 40 degrees incidence angle for ERS-1 and ERS-2 over time. Note the breakdown in calibration parameter calculation for ERS-2 after 2003. No intra-calibration was applied in the final implementation.

terized by fitting first-degree polynomials for each azimuth configuration. The resulting polynomials provide incidence-angle-dependent correction coefficients that are applied globally to adjust ERS-1 and ERS-2 backscatter measurements relative to the Metop-A ASCAT reference.

6. Results

6.1 Calibration Performance Assessment

Analysis of the uncalibrated ERS-1/2 ESCAT datasets reveals systematic discrepancies with Metop-A ASCAT observations. The scatter plots in Figures 5, 6, 7 and 8 demonstrate these differences through overlaying the parameterized correction functions with the underlying observation density distributions.

We note an incidence-angle dependent bias in ERS-1 and -2 backscatter measurements relative to the Metop-A ASCAT reference polynomial for both calibration and validation regions, ranging linearly from approximately 0.4 to -0.3 dB between 15° and 55° incidence angle.

After applying the derived calibration corrections, we observe substantial improvements in inter-instrument consistency, especially for descending orbits. Post-calibration analysis of validation regions demonstrates:

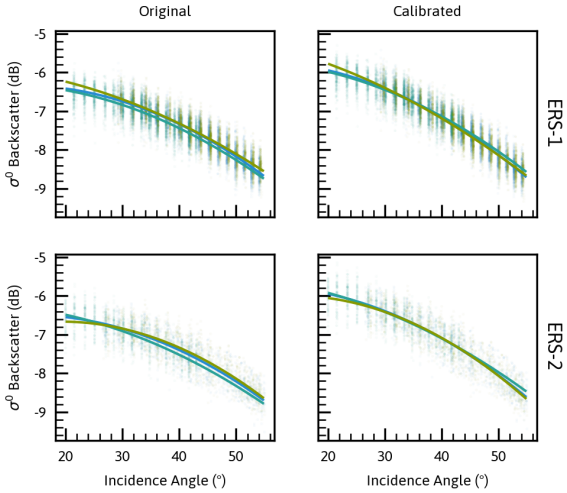

Figure 4. Improvement of beam agreement over SE Asia validation region after inter-calibration in both ERS-1 and ERS-2 (ascending orbits shown).

- The average bias between ERS-1/2 and Metop-A over validation regions is reduced for all azimuth configurations, with a remaining bias of approximately 0.1 dB at 40° incidence angle (approximately 0.12 dB for ascending orbits and 0.07 dB for descending orbits) for both satellites, due to the different incidence-angle response of the calibration regions compared to validation regions.
- Significantly reduced incidence angle dependency of inter-instrument bias in most azimuth configurations, indicating successful harmonization of the angular response characteristics between instruments, although due to regional differences, ERS-2 is slightly over-corrected in this regard.
- Improved beam-to-beam consistency within each ERS instrument, as demonstrated by reduced spread in the inter-beam comparisons (Figures 4).

7. Discussion

Application of Reimer’s 2014 rainforest-based inter-calibration methodology to the complete ERS dataset reveals that, thanks to good existing calibration during gyroscopically stable stages of ERS-1 and ERS-2, the original two-stage approach can be effectively simplified for the ASPS reprocessed data. Our experience indicates that focusing solely on inter-calibration relative to Metop-A ASCAT provides sufficient harmonization across the multi-mission record, while avoiding the added complexity and potential pitfalls of intra-calibration.

The decision to omit intra-calibration was based on careful analysis of the complete dataset. While this step theoretically provides benefits by removing temporal inconsistencies within individual missions, our analysis suggests that for most of the ASPS reprocessed data, these benefits are minimal relative to the added complexity and potential for over-correction. The inherent stability of the reprocessed dataset, combined with limited data availability for robust intra-calibration parameter estimation post-2003, made this adaptation both practical and justified.

This contribution has been peer-reviewed. The double-blind peer-review was conducted on the basis of the full paper.
https://doi.org/10.5194/isprs-annals-XI-3-2026-411-2026 | © Author(s) 2026. CC BY 4.0 License.

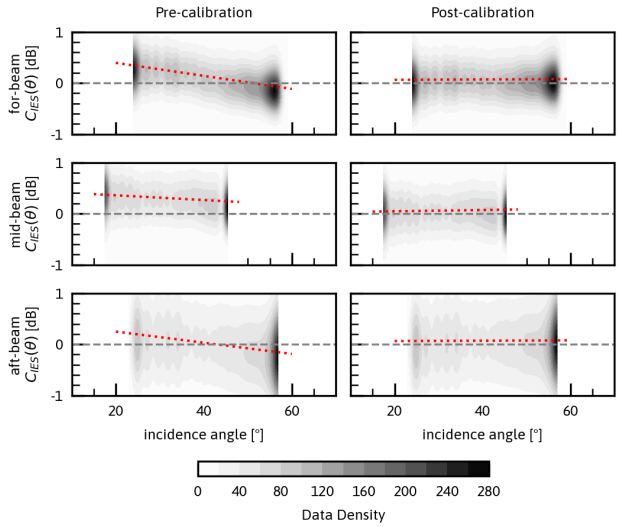

Figure 5. Inter-calibration coefficients correcting ERS-1 against Metop-A (dashed line) plotted over incidence angle before and after inter-calibration has been applied to the backscatter data. Density of ERS-1 observations behind. (Validation regions; descending orbits)

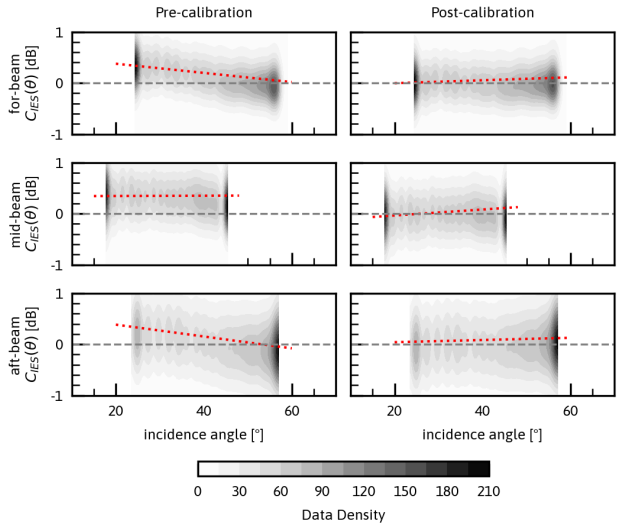

Figure 6. Same as Fig. 5 but for ERS-2.

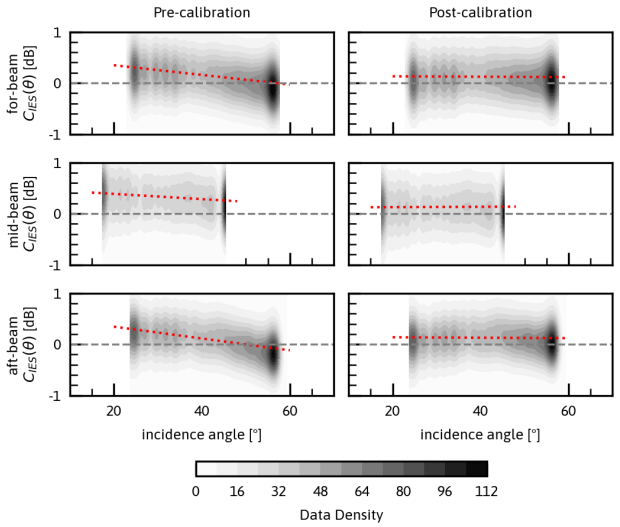

Figure 7. Inter-calibration coefficients correcting ERS-1 against Metop-A (dashed line) plotted over incidence angle before and after inter-calibration has been applied to the backscatter data. Density of ERS-1 observations behind. (Validation regions; ascending orbits)

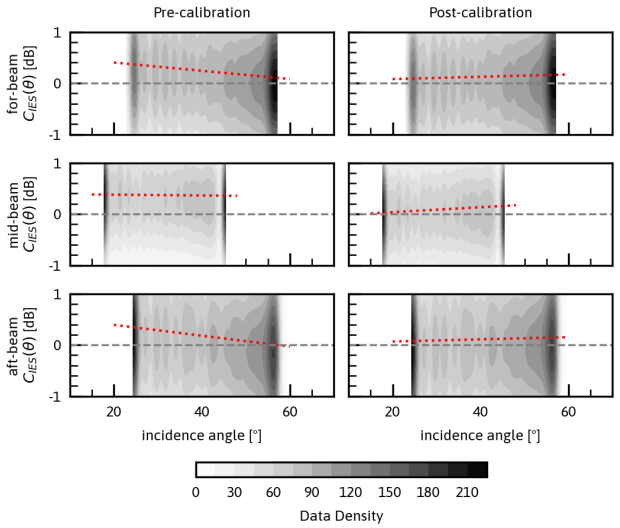

Figure 8. Same as Fig. 7 but for ERS-2.

Performance assessment indicates that the adapted approach achieves inter-mission consistency comparable to the original methodology, with systematic biases reduced to near-zero levels across the overlapping incidence angle range. Figure 4 demonstrates improved beam agreement within ERS instruments, while Figures 5 and 6 confirm successful harmonization with Metop-A ASCAT in independent validation regions.

However, several limitations must be acknowledged. The calibration approach is still fundamentally constrained by the quality and availability of reference data, particularly for ERS-2 post-2003 where tape recorder failure severely limits data coverage over calibration regions. The rainforest-based methodology may perform less optimally in regions or time periods where natural targets exhibit anomalous behavior due to unusual climatic conditions or vegetation stress. Additionally, the omission of intra-calibration, while justified for most of the record, means that some subtle temporal inconsistencies within individual missions may remain uncorrected.

8. Conclusions

This study demonstrates the successful practical implementation and adaptation of rainforest-based inter-calibration for creating a continuous C-band backscatter climate data record spanning the ERS and Metop missions. Our experience applying the established calibration methodology to the complete ERS dataset reveals several important findings:

- The original calibration methodology can be effectively implemented in a modern, open-source Python framework, providing both computational efficiency and community accessibility.

- For the ASPS reprocessed dataset, the intra-calibration step adds complexity without commensurate benefit, while inter-calibration alone provides sufficient cross-mission consistency.
- The complete ERS record, including previously unavailable ERS-1 data, can be successfully inter-calibrated with Metop-A ASCAT, creating a continuous dataset from 1991-present.

The resulting calibrated backscatter data record provides improved continuity for long-term environmental monitoring applications, particularly for soil moisture retrieval and vegetation dynamics studies, such as those ongoing within the FDR4LDYN (Fundamental Data Record for Land Dynamics) project (TU Wien et al., 2025). Our methodology also provides a practical framework for future scatterometer mission inter-calibration efforts.

Several limitations of this work warrant consideration for future research efforts. The primary constraint remains the incomplete treatment of ERS-2 data anomalies, particularly those occurring after the 2001 gyroscope failure and 2003-2004 tape recorder degradation. These anomalies affect a significant portion of the ERS-2 record and may require alternative calibration strategies or specialized correction approaches that were beyond the scope of this implementation.

Future research directions should therefore focus on: (1) developing robust calibration methods for the anomalously affected ERS-2 periods, potentially leveraging very stable points from several smaller rainforests for calibration; and (2) comprehensive validation of the calibrated dataset against independent observations and downstream applications, particularly soil moisture products where the enhanced continuity can be directly assessed.

Acknowledgements

This work was supported by the European Space Agency (FDR4LDYN, ESA Co. RFP/3-18440/24/I-DT-l).

References

Bartalis, Z., Wagner, W., Naeimi, V., Hasenauer, S., Scipal, K., Bonekamp, H., Figa, J., Anderson, C., 2007. Initial Soil Moisture Retrievals from the METOP-A Advanced Scatterometer (ASCAT). *Geophysical Research Letters*, 34(L20401).

Hahn, S., Harrison, C., 2025. TUW-GEO/fibgrid: V0.0.7. Zenodo.

Long, D., Skouson, G., 1996. Calibration of Spaceborne Scatterometers Using Tropical Rain Forests. *IEEE Transactions on Geoscience and Remote Sensing*, 34(2), 413–424.

Reimer, C., 2014. Calibration of Space-Borne Scatterometers : Towards a Consistent Climate Data Record for Soil Moisture Retrieval. Thesis, Technische Universität Wien.

Scipal, K., Wagner, W., Trommler, M., Naumann, K., 2002. The global soil moisture archive 1992-2000 from ERS scatterometer data: First results. 3, IEEE, 1399–1401.

TU Wien, TU Delft, European Space Agency, 2025. Fundamental data record for land dynamics (FDR4LDYN).

Wagner, W., Hahn, S., Kidd, R., Melzer, T., Bartalis, Z., Hasenauer, S., Figa-Saldaña, J., de Rosnay, P., Jann, A., Schneider, S., Komma, J., Kubu, G., Brugger, K., Aubrecht, C., Züger, J., Gangkofner, U., Kienberger, S., Brocca, L., Wang, Y., Blöschl, G., Eitzinger, J., Steinnocher, K., Zeil, P., Rubel, F., 2013. The ASCAT Soil Moisture Product: A Review of Its Specifications, Validation Results, and Emerging Applications. *Meteorologische Zeitschrift*, 22(1), 5–33.

Wagner, W., Lemoine, G., Borgeaud, M., Rott, H., 1999. A Study of Vegetation Cover Effects on ERS Scatterometer Data. *IEEE Transactions on Geoscience and Remote Sensing*, 37(2), 938–948.